APPLIED AND ENVIRONMENTAL MICROBIOLOGY, Mar. 1999, p. 989–994 Vol. 65, No. 3
0099-2240/99/$04.00+0

Steady-State Nitrogen Isotope Effects of N_2 and N_2O Production in *Paracoccus denitrificans*

CAROL C. BARFORD,[1]* JOSEPH P. MONTOYA,[2]† MARK A. ALTABET,[3] AND RALPH MITCHELL[1]

Division of Engineering and Applied Sciences[1] and Biological Laboratories,[2] Harvard University, Cambridge, Massachusetts 02138, and Center for Marine Science and Technology, University of Massachusetts, Dartmouth, North Dartmouth, Massachusetts 02747[3]

Received 21 August 1998/Accepted 4 December 1998

Nitrogen stable-isotope compositions ($\delta^{15}N$) can help track denitrification and N_2O production in the environment, as can knowledge of the isotopic discrimination, or isotope effect, inherent to denitrification. However, the isotope effects associated with denitrification as a function of dissolved-oxygen concentration and their influence on the isotopic composition of N_2O are not known. We developed a simple steady-state reactor to allow the measurement of denitrification isotope effects in *Paracoccus denitrificans*. With [dO_2] between 0 and 1.2 μM, the N stable-isotope effects of NO_3^- and N_2O reduction were constant at 28.6‰ ± 1.9‰ and 12.9‰ ± 2.6‰, respectively (mean ± standard error, $n = 5$). This estimate of the isotope effect of N_2O reduction is the first in an axenic denitrifying culture and places the $\delta^{15}N$ of denitrification-produced N_2O midway between those of the nitrogenous oxide substrates and the product N_2 in steady-state systems. Application of both isotope effects to N_2O cycling studies is discussed.

The importance of denitrification in microbial ecology, N_2O production, agricultural N loss and wastewater treatment has prompted a large body of research over the last 25 years. Although the basic pathway is well known (36),

$$NO_3^- \rightarrow NO_2^- \rightarrow NO \rightarrow N_2O \rightarrow N_2 \quad (1)$$

the regulation and distribution of denitrification remain poorly understood. The sensitivity of denitrification to oxygen tension is of particular interest due to (i) the recent demonstration of denitrification under aerobic conditions (40, 41), (ii) increased N_2O production under these conditions (12, 20, 28), (iii) the importance of linked nitrification-denitrification in N cycling in natural environments (11, 14), and (iv) development of "single-sludge" wastewater treatment as a low-cost alternative to traditional strategies that employ separate aerobic and anoxic reactors (26, 34, 47).

The natural-abundance ^{15}N ratios of nitrogenous materials have been used to identify or quantify denitrification activity in low-oxygen environments, including the marine water column (24, 53, 54, 55), groundwater (15), sediments (1), and soil (25). These studies exploit the variation in the ratio of ^{15}N to ^{14}N in nitrogenous material that results from the isotopic discrimination of denitrification, in which ^{14}N reacts faster than ^{15}N. Thus, natural-abundance ^{15}N ratios provide a small (≈0.366% ^{15}N) but endogenous in situ tracer of denitrification activity, in contrast to large ^{15}N additions (50 to 99% ^{15}N) traditionally used to trace biological N fixation and other N transformations. However, published estimates of the extent of isotopic discrimination, or isotope effect (ε), of denitrification range from 13 to 40‰, reflecting the variety of experimental methods and denitrifying cultures used (5, 6, 10, 13, 27, 50, 52). Because the ε of denitrification lies between those of other N transformations, such as N assimilation at 10‰ (9, 19, 30) and nitrification at 13 to 16‰ in situ (21) or 30 to 60‰ in vitro (27, 52), it is desirable that ε be better constrained. In addition, possible variation in ε as a function of oxygen tension has not been investigated heretofore.

We measured ε of denitrification in pure cultures of *Paracoccus denitrificans* under dissolved-oxygen concentrations between 0 and 1.2 μM. We also measured a unique ε for N_2O reduction in these cultures. For these experiments, we developed a simple, steady-state reactor which does not require a dedicated mass spectrometer or online sample preparation system, thus offering a flexible approach to investigators who do not routinely use stable-isotope techniques. The reactor was also used to measure oxygen isotope effects, which are reported elsewhere (4). This information expands the utility of stable isotope studies of denitrification in low-oxygen (<10 μM) environments. Here we describe the necessary steady-state fractionation models and the reactor configuration and performance and report the N stable-isotope effects for denitrification.

MATERIALS AND METHODS

Experimental design. Continuous cultures were used to control the dissolved-oxygen concentration ([dO_2]) more easily and to exploit the simplicity of steady-state fractionation models, which relate kinetic ε values directly to the isotopic compositions of reactants and products. The isotopic composition of nitrogenous material is commonly expressed as a δ-value relative to atmospheric N_2:

$$\delta^{15}N\ (‰) = [(R_{sample} - R_{N_2})/R_{N_2}] \times 1{,}000 \quad (2)$$

where $R = {}^{15}N/{}^{14}N$. In a single first-order reaction, in which the substrate pool is infinitely large, ε closely approximates the difference between the δ values of the substrate and product (16). The isotopic dynamics of steady-state anoxic denitrification may be idealized as such a one-step process:

$$\varepsilon_0 = \delta^{15}NO_3^- - \delta^{15}N_2 \quad (3)$$

where ε_0 is the overall ε of denitrification. Alternatively, this pseudo-ε may be partitioned:

$$\delta^{15}NO_3^- \xrightarrow{\varepsilon 1,\ \delta 1} \delta^{15}N_2O \xrightarrow{\varepsilon 2,\ \delta 2} \delta^{15}N_2 \quad (4)$$

where ε_1 and ε_2 are the ε values of NO_3^- and N_2O reduction, respectively, and δ_1 and δ_2 are the isotopic compositions of the instantaneous products of the two

* Corresponding author. Mailing address: Department of Earth and Planetary Sciences, Harvard University, 20 Oxford St., Cambridge, MA 02138. Phone: (617) 495-9624. Fax: (617) 495-2768. E-mail: ccb@io.harvard.edu.

† Present address: School of Biology, Georgia Institute of Technology, Atlanta, GA 30332.

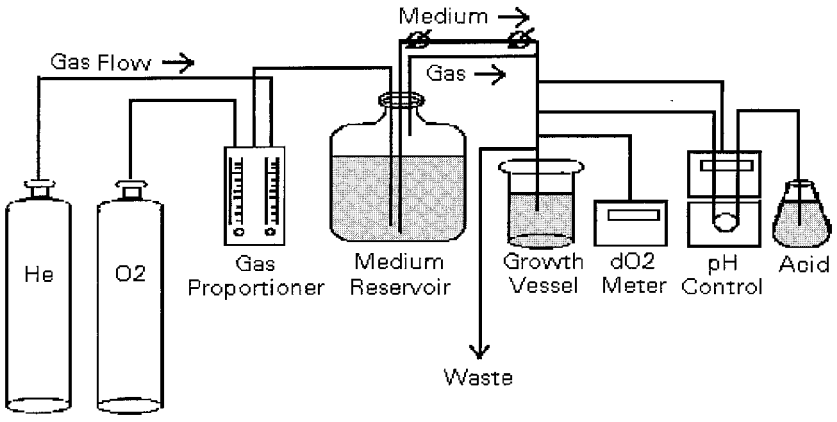

FIG. 1. Reactor configuration.

reactions. At steady state, $\delta^{15}N_2O$ and $\delta^{15}N_2$ are constant; thus, δ_1 and δ_2 both equal $\delta^{15}N_2$. Applying the principle of equation 3 to equation 4 yields the following relationships:

$$\varepsilon_1 = \delta^{15}NO_3^- - \delta_1 \quad (5a)$$

$$\varepsilon_2 = \delta^{15}N_2O - \delta_2 \quad (5b)$$

When $\delta^{15}NO_3^-$, $\delta^{15}N_2O$, and $\delta^{15}N_2$ are measured experimentally and $\delta^{15}N_2$ is substituted for δ_1 and δ_2, equations 5a and 5b may be solved for ε_1 and ε_2, respectively. Note that $\varepsilon_1 = \varepsilon_0$, which is generally true for unbranched, nonreversible reaction pathways (37).

The approach described above allows the calculation of ε_1 and ε_2 by measuring $\delta^{15}N$ of three species at a single steady state. Independent checks of ε_1 were calculated from isotopic mass balances of the reactor at multiple steady states. Because denitrification intermediates constituted very small fractions of reactor N at steady state, N isotope mass balances were written as follows:

$$D\,[NO_3^-]_i\delta^{15}N_i = D\,[NO_3^-]_{ss}\delta^{15}N_{ss} + R\,(\delta^{15}N_{ss} - \varepsilon_1) \quad (6)$$

where D is reactor dilution rate (time^{-1}), R is the denitrification rate ([N] time^{-1}), $\delta^{15}N$ is the δ value of NO_3^-, and the subscripts "i" and "ss" refer to initial and steady state, respectively. Equation 6, like equation 3, implies that ε_1 is equal to the steady-state difference between $\delta^{15}NO_3^-$ and $\delta^{15}N_2$. Because R equals the product of D and the concentration of substrate consumed in a continuous culture (chemostat) at steady state, equation 6 can be rewritten to eliminate R:

$$D\,[NO_3^-]_i\delta^{15}N_i = D\,[NO_3^-]_{ss}\delta^{15}N_{ss} + D\,([NO_3^-]_i - [NO_3^-]_{ss})\,(\delta^{15}N_{ss} - \varepsilon_1) \quad (7)$$

and may be rearranged into linear form:

$$\delta^{15}N_{ss} = \varepsilon_1([NO_3^-]_i - [NO_3^-]_{ss})/[NO_3^-]_i + \delta^{15}N_i \quad (8a)$$

$$\delta^{15}N_{ss} = \varepsilon_1(f) + \delta^{15}N_i \quad (8b)$$

where f is the fraction of NO_3^- consumed at steady state and ε_1 equals the slope of steady-state $\delta^{15}NO_3^-$ as a function of f (17). Different values of f were achieved by manipulating the dissolved-oxygen concentration ($[dO_2]$). Experimental $[dO_2]$ treatments were 0, 0.1, 0.3, and 1.2 μM.

Reactor configuration. The reactor system consisted of a medium reservoir, growth chamber, waste carboy, and connecting tubing and flow controls (Fig. 1). The 20-liter Pyrex carboy in which media were sterilized also served as the reservoir. A heavy-gauge aluminum lid and rubber gasket were secured to the reservoir with a collar and screws. The lid contained ports for gas entry, gas and medium exit to the growth chamber, and venting. Gas mixing and flow to the reservoir were controlled by a gas proportioner (Alltech, Deerfield, Ill.). Gas was conducted to the reservoir in 1/8-in. stainless steel tubing, through a 0.5-μm nominal matrix filter (Nupro, Willoughby, Ohio) and a sparging stone. Medium flow from the reservoir to the growth chamber was caused by positive pressure in the reservoir, which was in turn controlled by the sparging rate. Two needle valves (Nupro) were added to enable finer control of medium flow rate to the growth chamber. This mode of medium delivery was chosen over pumping due to the difficulty of maintaining absolutely anoxic connections between steel tubing and peristaltic pump tubing.

The growth chamber was a 2-liter Pyrex cylinder equipped with a magnetic stirrer and a stainless steel lid similar to the reservoir lid. In addition to gas and liquid entry ports, it contained a septum port for sampling by syringe, ports to accommodate a pH probe (Orion, Boston, Mass.), and a dO_2 probe (Ingold, Wilmington, Mass.), a 3/8-in. port for gas and liquid exit to the waste carboy, and a 3/8-in. port fitted with a shutoff valve for headspace sampling. The pH probe was connected to a pH controller (Cole Parmer, Chicago, Ill.), which activated a peristaltic pump equipped with microbore tubing to introduce HCl into the growth chamber. This tubing entered the growth chamber through the septum port. The waste port was situated to give the growth chamber a working volume of 1.75 liters. Waste liquid and gas were forced by positive pressure into the 20-liter vented waste carboy through 3/8-in. stainless steel tubing.

Organism and media. *P. denitrificans* ATCC 17741, a relatively oxygen-sensitive, classic denitrifier, was chosen for the experiments (2). Cultures were purchased from the American Type Culture Collection (Rockville, Md.) and reconstituted in nutrient broth (Difco, Detroit, Mich.) at 30°C. Subcultures were frozen in glycerol and stored at −20°C until needed. The defined medium for continuous-culture experiments contained 30 mM nitrate and 20 mM acetate, which was the sole electron donor, carbon source, and limiting substrate (39). The composition of denitrification medium was as follows (in grams per liter): KNO_3, 3.03; $CH_3COONa \cdot 3H_2O$, 2.72; K_2HPO_4, 0.8; KH_2PO_4, 0.3; NH_4Cl, 0.4; $MgSO_4 \cdot 7H_2O$, 0.4; trace-elements solution, 2 ml liter^{-1}. The trace-elements solution was modified from that of Vishniac and Santer (48) and contained (in grams per liter) EDTA, 50.0; $ZnSO_4$, 2.2; $CaCl_2$, 5.5; $MnCl_2 \cdot 4H_2O$, 5.06; $FeSO_4 \cdot 7H_2O$, 5.0; $(NH_4)_6Mo_7O_{24} \cdot 4H_2O$, 1.1; $CuSO_4 \cdot 5H_2O$, 1.57; $CoCl_2 \cdot 6H_2O$, 1.61.

Reactor operation and sampling. Denitrification medium was autoclaved in 16-liter batches at 121°C and 15 lb/in^2 for 80 min. Beginning immediately after sterilization, the reservoir was sparged with ultra-high-purity helium or O_2 in helium (Med-Tech Gases, Medford, Mass.). The growth chamber, dO_2 probe, liquid-sampling needle, waste vessel, and tubing were autoclaved and connected while hot. The pH probe was calibrated with standard buffers (Fisher Scientific, Fair Lawn, N.J.), surface sterilized with 70% ethanol, and inserted into the growth chamber. The chamber was filled to working volume with medium, which was sampled with a syringe when cool. The culture was then inoculated with 30 ml of stationary-phase *P. denitrificans* and grown in batch mode at 30°C to approximately 10^8 cells ml^{-1}. Medium was then added at an appropriate dilution rate, and the pH was maintained at 8.0 by automatic addition of 1 M HCl. The $[N_2O]$ of the headspace gas was monitored daily until it stabilized within a few ppm (by volume). At this point, the reactor was assumed to have reached steady state (see below).

Once steady state was established for a given experimental $[dO_2]$ treatment, samples of each type were taken in triplicate. Liquid samples were drawn with a syringe and processed for either dissolved inorganic nitrogen concentrations (DIN) or cell N analysis. Samples (10 ml) for DIN analyses were filtered through 0.2-μm-pore-size cartridges (Gelman, Ann Arbor, Mich.), split into subsamples, and frozen until analysis of DIN or $\delta^{15}N$. Unfiltered liquid samples for cell counts were preserved in 5% formalin and stored at 10°C until analysis. Unfiltered samples for direct cell N measurement were processed immediately after sampling, as described below.

Gas samples were collected in preevacuated, U-shaped Pyrex tubes (34-ml volume) fitted on either end with vacuum stopcocks (Ace Glass, Vineland, N.J.). For N_2 collection, the U-tubes were coupled to the gas-sampling port of the growth chamber by using compression fittings with Teflon front ferrules and nylon back ferrules (Swagelok, Solon, Ohio). Each N_2 collection tube contained several granules of silica gel for cryogenic absorption of N_2 gas (33). With the growth chamber waste vent closed, U-tubes were opened and flushed with outgoing headspace gas (100 ml min^{-1}) for at least 5 min. Each grab sample was then isolated by closing first the stopcock near the sampling port and then the outlet stopcock. This order was necessary to maintain atmospheric pressure and to enable back-calculation of the N_2 production rate. Samples were stored in U-tubes for up to 2 days until purified and used for manometric determination of N_2.

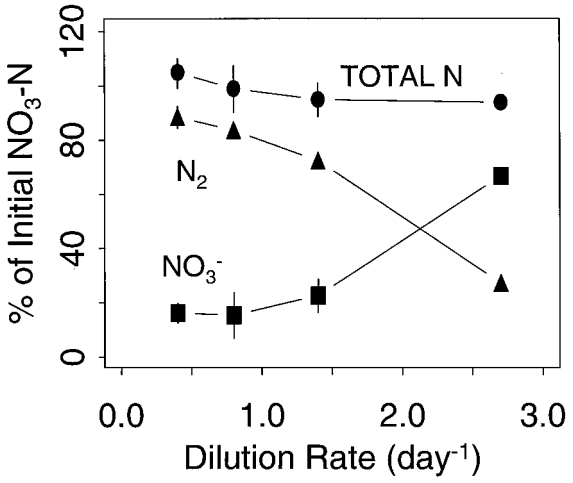

FIG. 2. Dissimilatory N budget as a function of the dilution rate. Symbols are means and SE ($n = 3$). NO_2^- and N_2O made up less than 1% of total N.

N_2O was quantified by gas chromatography. Samples for gas chromatography were collected by flushing a 30-ml serum bottle with outgoing headspace gas via the gas sampling port. N_2O samples for $\delta^{15}N$ and $\delta^{18}O$ determination were collected by trapping N_2O out of the outgoing gas stream. This was necessary because the headspace [N_2O] was too low (≈0.1 μM) for grab samples of reasonable volume to yield the 2 to 6 μmol of N required for mass spectrometry. The N_2O trap was a U-tube packed with borosilicate glass beads, which increased the trap surface area and dispersed the gas flow enough to trap N_2O when chilled in liquid nitrogen (LN_2). The efficiency of the N_2O trap was verified by measuring zero N_2O in the trap effluent. CO_2 was removed from N_2O samples by a scrubber in line between the growth chamber and the N_2O trap. The scrubber consisted of a standard gas purification cartridge (Alltech) packed with a 3-cm layer of Carbosorb granules (Elemental Microanalysis, Manchester, Mass.) between two layers of indicating silica gel.

Cryogenic distillation. Gas samples were purified by standard cryogenic techniques (7). U-tubes were first immersed in LN_2 to freeze the N_2 or N_2O sample onto silica gel or glass beads, respectively. The large overburden of helium carrier gas was then removed with a vacuum pump. N_2 samples were further purified of CO_2 and H_2O by a LN_2-cooled trap; O_2 was removed by passing the sample over copper filings at 550°C. The purified N_2 was quantified by using a capacitance manometer (MKS Baratron). N_2O samples were further purified of H_2O by using a glass trap cooled in an ethanol-dry ice slurry. Each N_2 or N_2O sample was refrozen in a Pyrex ampoule, sealed, and stored until analysis by continuous-flow isotope ratio mass spectrometry.

Analytical methods. Nitrate [NO_3^-] and nitrite [NO_2^-] concentrations were measured by the spongy cadmium reduction method (22). The ammonia [$NH_3 + NH_4^+$] concentration was determined by the colorimetric method of Strickland and Parsons (45). The $\delta^{15}N$ of ($NO_3^- + NO_2^-$) was measured by the ammonia diffusion method as modified by Sigman et al. (43).

The N in bacterial cells was quantified by acridine orange direct counting (18) and a conversion factor for cell N concentration, which was found by performing cell counting and direct cell N measurement on the same samples over a range of cell densities. Direct measurements of cell N were made with a Europa elemental analyzer. To prepare a sample containing 2 to 6 μmol of N, approximately 1.0 ml of cell suspension was filtered onto a precombusted 25-mm-diameter GF/F filter. The filters were dried at 55°C and packed in tin boats before analysis. Cell N was calculated from the following regression ($r^2 = 0.8835$, $n = 4$):

$$\text{Micrograms of cell N per milliliter} = 1.84 \times 10^{-8} (\text{cells per milliliter}) - 13.16 \quad (9)$$

N_2O production was monitored by using a Hewlett-Packard 5890A gas chromatograph equipped with an electron capture detector (23). A 1/8-in.-diameter stainless steel column packed with Hayesep Q 80/100 mesh was used at 40°C. The injector and detector temperatures were 100 and 350°C, respectively, and the carrier gas was 5% methane in argon at 30 ml min^{-1}. Under these conditions, N_2O eluted approximately 1.9 min after sample injection. Calibration curves were prepared daily by using a standard gas mixture of 101 ppm (volume) N_2O in N_2 (Scott Specialty Gases, Reading, Mass.). Standard injections were performed periodically to check for signal drift.

The $\delta^{15}N$ of N_2O, N_2, and ($NO_3^- + NO_2^-$) and the $\delta^{18}O$ of N_2O were measured on a Finnigan Mat 251 mass spectrometer (55). Samples were conducted by helium carrier flow (50 ml min^{-1}) through Carbosorb and magnesium perchlorate traps to remove trace CO_2 and H_2O, respectively. The mass 29/28 ratio was measured for N_2 samples and expressed as $\delta^{15}N$ relative to atmospheric N_2. Injections of working standard N_2 were made through a septum port in line with the carrier flow. For N_2O samples, the mass 45/44 ratio, yielding $\delta^{15}N$ values, and the mass 46/44 ratio, yielding $\delta^{18}O$ values, were both measured for each sample. The mass spectrometer was calibrated with a standard of pure N_2O gas kindly provided by T. Yoshinari, New York State Department of Health. N_2O δ values were expressed relative to the $\delta^{15}N$ and $\delta^{18}O$ of atmospheric N_2 and O_2, respectively.

Budget calculations. Dissimilatory (denitrification) and assimilatory N budgets were calculated for the reactor system. Each term in the dissimilatory budget was expressed as a percentage of the NO_3^- supplied in the medium:

$$\frac{[NO_3^-]_{ss}}{[NO_3^-]_i}(100\%) + \frac{[NO_2^-]_{ss}}{[NO_3^-]_i}(100\%) + \%\ N_2O_{ss} + \%\ N_{2ss} = \%\ \text{recovery} \quad (10)$$

The NO_3^- and NO_2^- terms were their respective steady-state concentrations (denoted by the subscript "ss") expressed as percentages of the initial NO_3^- concentration. The N_2O term ($\%N_2O_{ss}$) was the N_2O-N production rate expressed as a percentage of the NO_3^- supply rate:

$$\%\ N_2O_{ss} = \frac{(X_{N_2O})(\text{gas flow, liters/min})\left(\frac{1\ \text{mol}}{22.4\ \text{liters}}\right)\left(\frac{2N}{N_2O}\right)(100\%)}{([NO_3^-]_i, 1, \text{mol/liter})(\text{feed, liters/min})} \quad (11)$$

where X_{N_2O} is the mole fraction of N_2O in growth chamber headspace gas. The analogous N_2 term, $\%N_{2ss}$, is shown below. The first factor in this equation was the amount of N contained in a 34-ml grab sample, which was measured manometrically during cryogenic distillation:

$$\%\ N_{2ss} = \frac{\left(\frac{\mu g-\text{atoms of N}}{0.034\ \text{liter of sample}}\right)(\text{gas flow, liters/min})\left(\frac{1\ \text{mol}}{10^6\ \mu g-\text{atoms}}\right)(100\%)}{([NO_3^-]_i, \text{mol/liter})(\text{feed, liters/min})} \quad (12)$$

The assimilatory N budget consisted of the sum of cell N and NH_3-N present at steady state, expressed as a percentage of NH_3 supplied in the medium. Dissolved organic nitrogen compounds which may have been synthesized from NH_3 were not included in the budget.

RESULTS

Reactor performance. Dissimilatory N recovery from the reactor system was near 100% over a range of dilution rates (Fig. 2). Residual [NO_3^-] increased with increasing dilution rate, but the cultures were not in danger of washout at the rates tested (39). Dissimilatory N recovery varied as a function of the sparging rate (Fig. 3), with particularly high N_2 recovery at the lowest sparging rate, as discussed below. Assimilatory N recovery was 80 to 100% over the same range of dilution and sparging rates (data not shown). Dilution and sparging rates of 0.7 day^{-1} and 100 ml min^{-1}, respectively, were held constant in

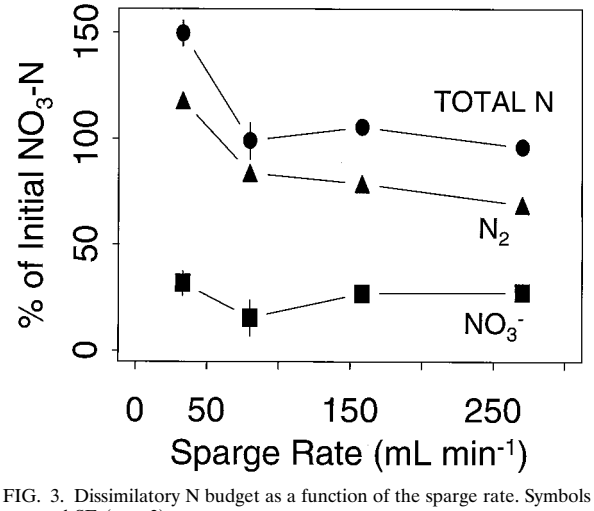

FIG. 3. Dissimilatory N budget as a function of the sparge rate. Symbols are means and SE ($n = 3$).

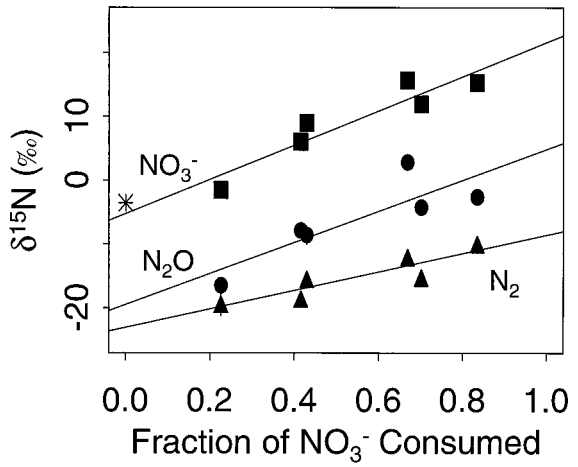

FIG. 4. $\delta^{15}N$ as a function of NO_3^- consumption (*f*). Different fractions of *f* were caused by dO_2 treatments. Symbols are means and SE ($n = 3$). The slope and SE of the slope of regressions of $\delta^{15}N$ versus *f* are 14.5 and 2.0 (N_2), 24.3 and 4.0 (N_2O), and 26.9 and 2.6 (NO_3^-). The asterisk represents the $\delta^{15}N$ of the NO_3^- supplied (−3.6‰).

further experiments, in which variable [dO_2] was the sole experimental treatment.

Experimental results. Under anoxic steady-state conditions, the reactor system yielded $\delta^{15}NO_3^-$, $\delta^{15}N_2O$, and $\delta^{15}N_2$ of 15.5‰ ± 0.3‰, 0.08‰ ± 3.1‰, and −11.0‰ ± 1.2‰, respectively (mean ± standard error [SE], $n = 6$). According to these data and equations, 5a and 5b, $\varepsilon_1 = 26.5‰ \pm 1.2‰$ and $\varepsilon_2 = 11.1‰ \pm 3.1‰$ under anoxic conditions. The independent estimates of ε_1 calculated from equation 8b and $\delta^{15}NO_3^-$ and $\delta^{15}N_2O$ from multiple steady states at different [dO_2] are similar although more variable (26.9‰ ± 2.6‰ and 24.3‰ ± 4.0‰, respectively). However, ε_1 calculated from $\delta^{15}N_2$ from multiple steady states was ≈14‰ (Fig. 4). This discrepancy and the high N_2 recovery at the low sparging rate (Fig. 3) suggested that significant isotopic signal from atmospheric N_2 had biased the $\delta^{15}N_2$ values. To quantify this bias, the response of measured $\delta^{15}N_2$ to systematic air contamination, or a "handling blank," was simulated (Fig. 5). The expected $\delta^{15}N_2$ was first calculated by subtracting the slope of the NO_3^- regression in Fig. 4 (i.e., ε_1) from points on that regression. The resulting straight line represents the $\delta^{15}N_2$ expected from constant fractionation and no air contamination. The expected $\delta^{15}N_2$ for the highest [dO_2] treatment (the least biogenic N_2) was compared to the measured value, and the amount of atmospheric N_2 necessary to create the difference was calculated by mass balance. Simulation of constant fractionation with constant air contamination was then made by adding the isotopic contribution of this amount (0.5 μmol) of atmospheric N_2 to the constant-fractionation values. The resulting curve fits very closely with the measured $\delta^{15}N_2$, suggesting that both ε_1 and the amount of air contamination during sampling were constant for all [dO_2] treatments.

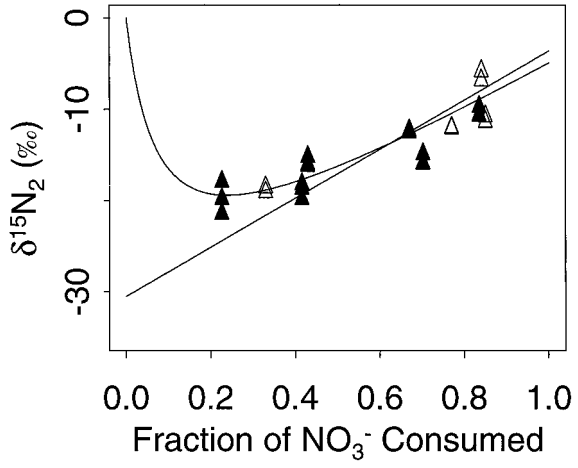

FIG. 5. Comparison between measured $\delta^{15}N_2$ from dO_2 experiments (solid triangles) and dilution rate experiments (open triangles), the expected $\delta^{15}N_2$ given constant fractionation (straight line), and the expected value with a constant amount of air contamination (curved line). See the text for details.

TABLE 1. Isotope effects for different dO_2 treatments, calculated from transformed $\delta^{15}N_2$

ε	ε^a at dO_2 of:					
	0 μM	0 μM	0.1 μM	0.1 μM	0.3 μM	1.2 μM
ε_1	29.3 ± 0.2a	26.6 ± 0.8b	28.8 ± 1.0a	29.7 ± 0.7a	28.7 ± 1.1a	12.4 ± 54[b]
ε_2	16.5 ± 0.8c	8.6 ± 0.9d	11.3 ± 1.7e	13.5 ± 0.9f	14.7 ± 1.3cf	−2.6 ± 54[b]

[a] Data are means ± SE ($n = 3$). Means sharing a letter are not significantly different ($P < 0.05$) according to the least-significant-difference test for planned comparisons (44). Columns of data with the same dO_2 concentration represent results of different runs.
[b] See the text.

To compare ε_1 and ε_2 between dO_2 treatments, the $\delta^{15}N_2$ data were transformed to eliminate the effect of air contamination. This was done by subtracting from each measured $\delta^{15}N_2$ value the isotopic bias inherent in 0.5 μmol of atmospheric N_2. The corrected $\delta^{15}N_2$ values for each treatment were then averaged, and these means were subtracted from the corresponding mean values of $\delta^{15}NO_3^-$ and $\delta^{15}N_2O$ to yield ε_1 and ε_2, respectively (Table 1). Analysis of variance indicates that ε_1 and ε_2 varied more between reactor runs than between [dO_2] treatments. The 1.2 μM dO_2 treatment was excluded from the analysis of variance because low biogenic N_2 production made $\delta^{15}N_2$ very sensitive to the mass balance correction (Table 1). Given the supporting evidence for systematic air contamination and the good agreement between intratreatment estimates of ε_1 and regression models of intertreatment $\delta^{15}N_2O$ and $\delta^{15}NO_3^-$ (Fig. 4), ε_1 and ε_2 were assumed to be constant over the range of dO_2 treatments and are reported as the grand means 28.6‰ ± 1.9‰ and 12.9‰ ± 2.6‰, respectively (means ± SE, $n = 5$).

TABLE 2. Measured values of the overall isotope effect of denitrification

Experimental system	ε (‰)	Reference
Pseudomonas denitrificans	13–21	13
Pseudomonas stutzeri	20–30	50
Nitrosomonas europaea[a]	35–36	52
Soil (amended with glucose)	14–23	5
Soil (unamended) at 20°C	29.4 ± 2.4	27
Soil (unamended) at 30°C	24.6 ± 0.9	27
Eastern tropical North Pacific	30–40	10
Groundwater	15.9	6

[a] Assumes that N_2O is formed by NO_2^- reduction.

DISCUSSION

The value of ε_1 reported here falls well within the range in the literature (Table 2). All estimates of biological fractionation are well below 90‰, the maximum theoretical fractionation of N—O bond rupture (50). The precision of ε_1 as measured in our steady-state system compares favorably with that measured by batch culture experiments (5, 13), in which ε_1 was calculated by using the classic Rayleigh equation, which is sensitive to error in f (46). The value and precision of ε_1 are similar to those reported by Mariotti et al. (27), who measured f by the acetylene block technique.

The results reported here indicate that ε_1 in *P. denitrificans* is constant over a range of dO_2 concentrations. This constancy supports the validity of using ε_1 to quantify, identify, or rule out denitrification fluxes in environments containing $[dO_2]$ gradients. However, other work indicates that biological kinetic fractionation can vary with environmental conditions. For sulfate reduction, Rees (38) hypothesized that the greater fractionation often measured in situ is due to slower growth in the field than in pure culture, but our dilution rate experiments indicated that the growth rate per se did not cause ε_1 to vary (Fig. 5). Bryan et al. (8) showed that the overall ε of denitrification does vary with the denitrification rate in whole cells and cell extracts of *Pseudomonas stutzeri* limited by $[NO_2^-]$, increasing to a maximum value of 25‰ ± 3.2‰ at initial $[NO_2^-] > 2.5$ mM. The electron acceptor concentrations in our experiments were well within the asymptotic range reported by Bryan et al. (above 2.5 mM). These authors also found a negative correlation between ε and denitrification rate when the rate was increased by higher electron donor concentrations.

The isotopic composition of N_2O in our experiments was quite distinct from both $\delta^{15}N_2$ and $\delta^{15}NO_3^-$. The combined effects of ε_1 and ε_2 resulted in $\delta^{15}N_2O$ being about 13‰ heavier and 15‰ lighter than $\delta^{15}N_2$ and $\delta^{15}NO_3^-$, respectively, at steady state. To our knowledge, this is the first report of an isotope effect for nitrous oxide reduction in a denitrifying system. Yoshida et al. (53) cited unpublished data which yielded a value of 27‰ for ε_2 in *P. denitrificans*, but they did not specify whether the bacteria were supplied with N_2O, NO_2^-, or NO_3^-. Yamazaki et al. (51) reported a maximum ε of 39‰ for N_2O reduction by the N_2 fixer *Azotobacter vinelandii*, but nitrogenase, not nitrous oxide reductase, appeared to be responsible for the observed activity.

The expression of isotopic fractionation by *P. denitrificans* was strongly influenced by $[dO_2]$. Within the narrow range between 0 and slightly more than 1.2 μM dO_2, the $\delta^{15}N$ of NO_3^- and N_2O varied up to 26‰ and $\delta^{15}N_2$ probably varied to an equal extent (Fig. 4). However, the usefulness of $[dO_2]$ as a predictor of $\delta^{15}N$ in denitrifying environments may be limited to the extent to which it controls NO_3^- consumption. The expression of ε in natural and applied systems will also depend on the distribution of denitrifiers. *P. denitrificans* is very sensitive to dO_2 in comparison to some denitrifiers, such as *Comamonas* sp. (35) and *Thiosphaera pantotropha* (39), which under aerobic conditions maintain 40 and 25% of their anaerobic denitrifying activity, respectively. However, *Pseudomonas fluorescens*, which frequently dominates denitrifying environments, denitrifies over approximately the same range of $[dO_2]$ as *P. denitrificans* (28). Chemostat studies of *P. halodenitrificans* revealed only slightly higher tolerance to dO_2, to ~2 μM (20).

It is hoped that ε_1 and ε_2 may be used to help distinguish between denitrification and nitrification as sources of N_2O and may serve as in situ tracers of both processes. For example, if the $\delta^{15}N$ of the substrate pools for both processes, NO_3^- and NH_4^+, respectively, are assumed to be zero, then denitrification- and nitrification-produced $\delta^{15}N_2O$ in open systems at steady state would be ca. −15‰ and −65‰, respectively (52). However, the isotopic composition of substrate pools in real systems could obscure this distinction. The $\delta^{15}N$ of NO_3^- and NH_4^+ vary from −23 to +43‰ and −20 to +50‰, respectively, depending upon the source and the combined fractionation effects of redox reactions in the environment (49). Given these ranges, it is possible that denitrification- and nitrification-produced $\delta^{15}N_2O$ would be indistinguishable. Linked nitrification-denitrification may also confuse $\delta^{15}N_2O$ signatures by increasing the range of potential substrate molecules, which may in turn may have variable $\delta^{15}N$ (56). In environments such as sediments and biofilms, spatial linkage between nitrification and denitrification is on the order of 1 mm or less, and in single microorganisms such as *Thiosphaera pantotropha*, which both denitrifies and nitrifies in aerobic environments, N_2O may be produced from NH_4^+, NO_3^-, and NO_2^- (3). However, in many environments (9, 19, 29, 31), the $\delta^{15}N$ of substrate pools can be constrained within a range of 10‰ (see, e.g., references 1, 32, and 42), and the isotopic composition of N_2O could provide a simple index to the relative contribution of the two processes producing N_2O.

ACKNOWLEDGMENTS

We thank J. Nevins for generous technical assistance and M. Hullar and J.-D. Gu for helpful discussion.

This work was supported in part by NASA NAG 2-843 (awarded to R.M.), NSF OCE-95-30187 and NSF DEB-96-33510 (awarded to J.P.M.), and NSF OCE-95-26356 (awarded to M.A.A.).

REFERENCES

1. **Altabet, M. A., R. Francois, D. W. Murray, and W. L. Prell.** 1995. Climate-related variations in denitrification in the Arabian Sea from sediment $^{15}N/^{14}N$ ratios. Nature **373:**506–509.
2. **Aragno, M., and H. G. Schlegel.** 1981. The hydrogen-oxidizing bacteria, p. 865–893. *In* M. P. Starr, H. Stolp, H. G. Trüper, A. Balows, and H. G. Schlegel (ed.), The prokaryotes. Springer-Verlag, New York, N.Y.
3. **Arts, P. A. M., L. A. Robertson, and J. G. Kuenen.** 1995. Nitrification and denitrification by *Thiosphaera pantotropha* in aerobic chemostat cultures. FEMS Microbiol. Ecol. **18:**305–316.
4. **Barford, C. C.** 1997. Ph.D. thesis. Harvard University, Cambridge, Mass.
5. **Blackmer, A. M., and J. M. Bremner.** 1977. Nitrogen isotope discrimination in denitrification of nitrate in soils. Soil Biol. Biochem. **9:**73–77.
6. **Böttcher, J., O. Strebel, S. Voerkelius, and H.-L. Schmidt.** 1990. Using isotope fractionation of nitrate-nitrogen and nitrate-oxygen for evaluation of microbial denitrification in a sandy aquifer. J. Hydrol. **114:**413–424.
7. **Boutton, T. W.** 1991. Stable carbon isotope ratios of natural materials. I. Sample preparation and mass spectrometric analysis, p. 155–171. *In* D. C. Coleman and B. Fry (ed.), Carbon isotope techniques. Academic Press, Ltd., London, United Kingdom.
8. **Bryan, B. A., G. Shearer, J. L. Skeeters, and D. H. Kohl.** 1983. Variable expression of the nitrogen isotope effect associated with denitrification of nitrite. J. Biol. Chem. **258:**8613–8617.
9. **Cifuentes, L. A., M. L. Fogel, J. R. Pennock, and J. H. Sharp.** 1989. Biogeochemical factors that influence the stable isotope ratio of dissolved ammonium in the Delaware Estuary. Geochim. Cosmochim. Acta **53:**2713–2721.
10. **Cline, J. D., and I. R. Kaplan.** 1975. Isotopic fractionation of dissolved nitrate during denitrification in the eastern tropical North Pacific Ocean. Marine Chem. **3:**271–299.
11. **Codispoti, L. A., and J. P. Christensen.** 1985. Nitrification, denitrification and nitrous oxide cycling in the eastern tropical South Pacific Ocean. Marine Chem. **16:**277–300.
12. **Davies, K. J. P., D. Lloyd, and L. Boddy.** 1989. The effect of oxygen on denitrification in *Paracoccus denitrificans* and *Pseudomonas aeruginosa*. J. Gen. Microbiol. **135:**2445–2451.
13. **Delwiche, C. C., and P. L. Steyn.** 1970. Nitrogen isotope fractionation in soils and microbial reactions. Environ. Sci. Technol. **4:**929–935.
14. **Devol, A. H., and J. P. Christensen.** 1993. Benthic fluxes and nitrogen cycling in sediments of the continental margin of the eastern North Pacific. J. Marine Res. **51:**345–372.
15. **Durka, W., E.-D. Schulze, G. Gebauer, and S. Voerkelius.** 1994. Effects of forest decline on uptake and leaching of deposited nitrate determined from

^{15}N and ^{18}O measurements. Nature **372:**765–767.
16. **Goericke, R., J. P. Montoya, and B. Fry.** 1994. Physiology of isotopic fractionation in algae and cyanobacteria, p. 187–221. *In* K. Lajtha and R. H. Michener (ed.), Stable isotopes in ecology and environmental science. Blackwell Scientific Publications, Cambridge, Mass.
17. **Hayes, J. M.** 1982. Fractionation *et al.*: an introduction to isotopic measurements and terminology. Spectra **8:**3–8.
18. **Hobbie, J. E., R. J. Daley, and S. Jasper.** 1977. Use of Nuclepore filters for counting bacteria by fluorescence microscopy. Appl. Environ. Microbiol. **33:** 1225–1228.
19. **Hoch, M. P., M. L. Fogel, and D. L. Kirchman.** 1994. Isotope fractionation during ammonium uptake by marine microbial assemblages. Geomicrobiol. J. **12:**113–127.
20. **Hochstein, L. I., M. Betlach, and G. Kritikos.** 1984. The effect of oxygen on denitrification during steady-state growth of *Paracoccus halodenitrificans*. Arch. Microbiol. **137:**74–78.
21. **Horrigan, S. G., J. P. Montoya, J. L. Nevins, and J. J. McCarthy.** 1990. Natural isotopic composition of dissolved inorganic nitrogen in the Chesapeake Bay. Estuarine Coastal Shelf Sci. **30:**393–410.
22. **Jones, M. N.** 1984. Nitrate reduction by shaking with cadmium. Alternative to cadmium columns. Water Res. **18:**643–646.
23. **Kaspar, H. F., and J. M. Tiedje.** 1980. Response of electron-capture detector to hydrogen, oxygen, nitrogen, carbon dioxide, nitric oxide and nitrous oxide. J. Chromatogr. **193:**142–147.
24. **Kim, K.-R., and H. Craig.** 1990. The two-isotope characterization of N_2O in the Pacific Ocean and constraints on its origin in deep water. Nature **347:**58–61.
25. **Kim, K.-R., and H. Craig.** 1993. Nitrogen-15 and oxygen-18 characteristics of nitrous oxide: a global perspective. Science **262:**1855–1857.
26. **Kuenen, J. G., and L. A. Robertson.** 1994. Combined nitrification-denitrification processes. FEMS Microbiol. Rev. **15:**109–118.
27. **Mariotti, A., J. C. Germon, P. Hubert, P. Kaiser, R. Letolle, A. Tardieux, and P. Tardieux.** 1981. Experimental determination of nitrogen kinetic isotope fractionation: some principles; illustration for the denitrification and nitrification processes. Plant Soil **62:**413–430.
28. **McKenney, D. J., C. F. Drury, W. I. Findlay, B. Mutus, T. McDonnell, and C. Gajda.** 1994. Kinetics of denitrification by *Pseudomonas fluorescens*: oxygen effects. Soil Biol. Biochem. **26:**901–908.
29. **Montoya, J. P., S. G. Horrigan, and J. J. McCarthy.** 1990. Natural abundance of ^{15}N in particulate nitrogen and zooplankton in the Chesapeake Bay. Mar. Ecol. Prog. Ser. **65:**35–61.
30. **Montoya, J. P., and J. J. McCarthy.** 1995. Nitrogen isotope fractionation during nitrate uptake by marine phytoplankton in continuous culture. J. Plankton Res. **17:**439–464.
31. **Nadelhoffer, K. J., and B. Fry.** 1994. Nitrogen isotope studies in forest ecosystems, p. 22–44. *In* K. Lajtha and R. H. Michener (ed.), Stable isotopes in ecology and environmental science. Blackwell Scientific Publications, Cambridge, Mass.
32. **Naqvi, S. W. A., T. Yoshinari, D. A. Jayakumar, M. A. Altabet, P. V. Narvekar, A. H. Devol, J. A. Brandes, and L. A. Codispoti.** 1998. Budgetary and biogeochemical implications of N_2O isotope signatures in the Arabian Sea. Nature **394:**462–464.
33. **Nevins, J. L., M. A. Altabet, and J. J. McCarthy.** 1985. Nitrogen isotope ratio analysis of small samples: sample preparation and calibration. Anal. Chem. **57:**2143–2145.
34. **O'Neill, M., and N. J. Horan.** 1995. Achieving simultaneous nitrification and denitrification of wastewaters at reduced cost. Water Sci. Technol. **32:**303–312.
35. **Patreau, D., N. Bernet, and R. Moletta.** 1996. Effect of oxygen on denitrification in continuous chemostat culture with *Comamonas* sp SGLY2. J. Ind. Microbiol. **16:**124–128.
36. **Payne, W. J.** 1973. Reduction of nitrogenous oxides by microorganisms. Microbiol. Rev. **37:**409–452.
37. **Peterson, B. J., and B. Fry.** 1987. Stable isotopes in ecosystem studies. Annu. Rev. Ecol. Syst. **18:**293–320.
38. **Rees, C. E.** 1973. A steady-state model for sulphur isotope fractionation in bacterial reduction processes. Geochim. Cosmochim. Acta **37:**1141–1162.
39. **Robertson, L. A.** 1988. Aerobic denitrification and heterotrophic nitrification in *Thiosphaera pantotropha* and other bacteria. Ph.D. thesis. Technical University of Delft, Delft, The Netherlands.
40. **Robertson, L. A., and J. G. Kuenen.** 1984. Aerobic denitrification: a controversy revived. Arch. Microbiol. **139:**351–354.
41. **Robertson, L. A., E. W. J. van Neil, R. A. M. Torremans, and J. G. Kuenen.** 1988. Simultaneous nitrification and denitrification in aerobic chemostat cultures of *Thiosphaera pantotropha*. Appl. Environ. Microbiol. **54:**2812–2818.
42. **Schäfer, P., and V. Ittekkot.** 1993. Seasonal variability of $\delta^{15}N$ in settling particles in the Arabian Sea and its palaeogeochemical significance. Naturwissenschaften **80:**511–513.
43. **Sigman, D. M., M. A. Altabet, R. Michener, D. C. McCorkle, B. Fry, and R. M. Holmes.** 1997. Natural abundance-level measurement of the nitrogen isotopic composition of oceanic nitrate: an adaptation of the ammonia diffusion method. Marine Chem. **57:**227–242.
44. **Sokal, R. R., and F. J. Rohlf.** 1995. Biometry. W. H. Freeman & Co., New York, N.Y.
45. **Strickland, J. D. H., and T. R. Parsons.** 1968. A practical handbook of seawater analysis. Fisheries Research Board of Canada, Ottawa, Canada.
46. **Tong, J. Y., and P. E. Yankwich.** 1957. Calculation of experimental isotope effects for pseudo first-order irreversible reactions. J. Phys. Chem. **61:**540–543.
47. **U.S. Environmental Protection Agency.** 1993. Nitrogen control. Publication EPA/625/R-93/010. U.S. Environmental Protection Agency, Washington, D.C.
48. **Vishniac, W., and M. Santer.** 1957. The thiobacilli. Bacteriol. Rev. **21:**195–213.
49. **Wada, E., and A. Hattori.** 1991. Nitrogen in the sea: forms, abundances, and rate processes. CRC Press, Inc., Boca Raton, Fla.
50. **Wellman, R. P., F. D. Cook, and H. R. Krouse.** 1968. Nitrogen-15: microbiological alteration of abundance. Science **161:**269–270.
51. **Yamazaki, T., N. Yoshida, E. Wada, and S. Matsuo.** 1987. N_2O reduction by *Azotobacter vinelandii* with emphasis on kinetic nitrogen isotope effects. Plant Cell Physiol. **28:**263–271.
52. **Yoshida, N.** 1988. ^{15}N-depleted N_2O as a product of nitrification. Nature **335:**528–529.
53. **Yoshida, N., A. Hattori, T. Saino, S. Matsuo, and E. Wada.** 1984. $^{15}N/^{14}N$ ratio of dissolved N_2O in the eastern tropical Pacific Ocean. Nature **307:**442–444.
54. **Yoshida, N., H. Morimoto, M. Hirano, I. Koike, S. Matsuo, E. Wada, T. Saino, and A. Hattori.** 1989. Nitrification rates and ^{15}N abundances of N_2O and NO_3^- in the western North Pacific. Nature **342:**895–897.
55. **Yoshinari, T., M. A. Altabet, S. W. A. Naqvi, L. Codispoti, A. Jayakumar, M. Kuhland, and A. Devol.** 1997. Nitrogen and oxygen isotopic composition of N_2O from suboxic waters of the eastern tropical North Pacific and the Arabian Sea - measurement by continuous-flow isotope-ratio monitoring. Marine Chem. **56:**253–264.
56. **Yoshinari, T., and I. Koike.** 1994. The use of stable isotopes for the study of gaseous nitrogen species in marine environments, p. 114–137. *In* K. Lajtha and R. H. Michener (ed.), Stable isotopes in ecology and environmental science. Blackwell Scientific Publications, Cambridge, Mass.